Possible magnetic order and suppression of superconductivity by V doping in Sr$_2$VO$_3$FeAs

Marcus Tegel,[1] Tanja Schmid,[1] Tobias Stürzer,[1] Masamitsu Egawa,[1] Yixi Su,[2] Anatoliy Senyshyn,[3] and Dirk Johrendt[1,*]

[1]*Department Chemie, Ludwig-Maximilians-Universität München, Butenandtstraße 5-13 (Haus D), 81377 München, Germany*
[2]*Jülich Centre for Neutron Science, IFF, Forschungszentrum Jülich, Outstation at FRM II, Lichtenbergstraße 1, 85747 Garching, Germany*
[3]*Institute for Materials Science, Darmstadt University of Technology, 64287 Darmstadt, Germany*

Superconductivity at 33 K in Sr$_2$VO$_3$FeAs is completely suppressed by small amounts of V doping in Sr$_2$VO$_3$(Fe$_{0.93(\pm0.01)}$V$_{0.07(\pm0.01)}$)As. The crystal structures and exact stoichiometries are determined by combined neutron powder diffraction and x-ray powder diffraction. Sr$_2$VO$_3$FeAs is shown to be very sensitive to Fe/V mixing, which interferes with or even suppresses superconductivity. This inhomogeneity may be intrinsic and explains scattered reports regarding T_c and reduced superconducting phase fractions in Sr$_2$VO$_3$FeAs. Neutron-diffraction data collected at 4 K indicate incommensurate magnetic ordering of the V sublattice with a propagation vector $\mathbf{q} \approx (0,0,0.306)$. This suggests strongly correlated vanadium, which does not contribute significantly to the Fermi surface of Sr$_2$VO$_3$FeAs.

The discovery of iron pnictide superconductors[1–3] has opened a new chapter in superconductor research. Enormous progress has already been made with respect to the physics of these materials and it becomes increasingly accepted that the weak magnetism inside the iron layers plays a decisive role in superconductivity,[4] even though the specific relationship to the pairing mechanism is still unclear. This weak magnetism appears as a spin-density wave (SDW) in all iron-based materials with simple PbFCl- (Refs. [5] and [6]) and ThCr$_2$Si$_2$-related structures[7] and is intimately connected with nesting of cylinder-shaped Fermi surfaces by a wave vector $\mathbf{q} = (\pi, \pi)$.[8] However, no SDW of that or similar kind has been observed in the more complex arsenides Sr$_2$MO$_3$FeAs (M = Sc, Cr, V) (Refs. [9–11]) where the isoelectronic (FeAs)$^{1-}$ layers are separated by larger perovskitelike (Sr$_2$MO$_3$)$^{1+}$ blocks. Among them, only the V compound Sr$_2$VO$_3$FeAs is superconducting up to 37 K (Ref. [11]) and it has been controversially argued whether in this case the V atoms significantly contribute to the Fermi surface[12] or not.[13] If this is not the case, the topology of the Fermi surface turns out to have the same essential features as in the other FeAs superconductors, otherwise one has to assume another mechanism in the case of Sr$_2$VO$_3$FeAs. The latter seems to be improbable with respect to the T_c, which is strikingly similar to other iron arsenide superconductors.

If we assume for the moment that the superconducting mechanism in Sr$_2$VO$_3$FeAs is the same as in the other iron arsenides, the absence of any SDW anomaly may suggest that the FeAs layer is intrinsically doped. Vanadium can easily adopt oxidation states between V^{1+} and V^{4+} and would thus be able to supply or to accept electrons from the FeAs layers. Indeed, a recent x-ray absorption study indicates the presence of V^{3+} and V^{4+} in a Sr$_2$VO$_3$FeAs sample.[14] But even in this case, it remains confusing that also Sr$_2$ScO$_3$FeAs, where the scandium valence is fixed to Sc^{3+}, shows neither a SDW nor any other magnetic effect.[9]

However, thorough investigations of Sr$_2$VO$_3$FeAs are hampered by the poor quality of the samples, which always contain significant amounts of the ternary vanadium oxides Sr$_2$VO$_4$ and/or Sr$_3$V$_2$O$_{7-\delta}$.[11,14,15] However, quantitative phase fractions are not specified by the authors. This might be dangerous in the present case because these impurities contain V^{4+} and exhibit at least weak paramagnetism.

Another fact that is hardly noticed so far concerns the true stoichiometry and homogeneity of the Sr$_2$MO$_3$FeAs compounds. The ionic radii of Fe^{2+}, V$^{2+/3+}$, and Cr^{3+} are similar and in face of synthesis temperatures above 1000 °C, their mixing is easily conceivable. Indeed, we have recently found by neutron diffraction that the chromium compound Sr$_2$CrO$_3$FeAs is not stoichiometric but intrinsically Cr doped in the iron layer.[16] We suggest that this mixing probably poisons superconductivity. Such mixing of iron and vanadium can also occur in Sr$_2$VO$_3$FeAs and already small amounts of V in the Fe layer may seriously affect the electronic and magnetic properties.

In order to shed some light on this puzzling material, we have optimized the synthesis of Sr$_2$VO$_3$FeAs in order to minimize the amounts of impurity phases, which allowed us to perform combined x-ray and neutron-powder scattering investigations. In this Rapid Communication, we report on the exact stoichiometry, magnetism, and superconductivity of differently prepared Sr$_2$VO$_3$FeAs samples. We show that the superconducting phase is almost ideally stoichiometric, whereas small V doping, which can easily be achieved in the Fe layer, suppresses superconductivity. We present susceptibility data and discuss hints to magnetic ordering of the V sublattice from neutron-scattering data.

Sr$_2$VO$_3$FeAs was synthesized by heating mixtures of strontium, vanadium, iron (III) oxide, and arsenic oxide in a molar ratio of 20:11:5:5. Two separate batches of 1 g were prepared in alumina crucibles sealed in silica ampoules under an atmosphere of purified argon. Each mixture was heated to 1323 K at a rate of 60 K/h, kept at this temperature for 60 h and cooled down to room temperature. The products were homogenized in an agate mortar, pressed into pellets, and sintered at 1323 K for 60 h. The latter step was performed twice. The batches were then united, reground, pressed into pellets of 6 mm in diameter, and sintered together at 1323 K for 68 h. The obtained black crystalline product Sr$_2$VO$_3$FeAs is stable in air. Sr$_2$VO$_3$(Fe$_{0.93}$V$_{0.07}$)As
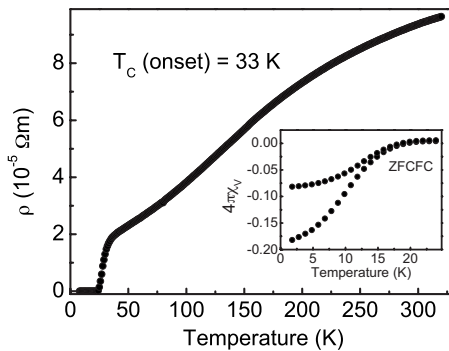
FIG. 1. Resistivity of Sr_2VO_3FeAs. Inset: zero-field-cooled/field-cooled measurements (20 Oe).

was synthesized by heating mixtures of strontium, vanadium, iron (III) oxide, arsenic oxide, and vanadium (V) oxide in a ratio of 100:54:20:25:3 in two separate batches accordingly.

Resistivity measurements of the undoped sample show a rather broad superconducting transition at 33 K (Fig. 1). Superconductivity is verified by the zero-field-cooled/field-cooled measurements using a Quantum Design superconducting quantum interference device magnetometer, however, the estimated superconducting-volume fraction is only 20%. No superconductivity is detected in the V-doped sample. The susceptibilities of V-doped and undoped Sr_2VO_3FeAs measured at 1000 Oe and hysteresis loops at different temperatures are depicted in Fig. 2. Both samples exhibit Curie-Weiss-type paramagnetic behavior between 160 and 390 K. Anomalies appear at ≈ 150, ≈ 70, and ≈ 50 K in the stoichiometric sample and similar also in the V-doped sample. Almost the same behavior has recently been reported in Ref. 14, where the authors suggest possible magnetic transitions of the Sr_2VO_3 layers and the absence of a structural transition both in agreement with our neutron-scattering results (see below).

X-ray powder-diffraction patterns at room temperature were recorded using a STOE STADI P diffractometer (Cu $K_{\alpha 1}$, $\lambda = 0.154056$ nm). Neutron powder-diffraction patterns at 300 K and 4 K were recorded at the high-resolution
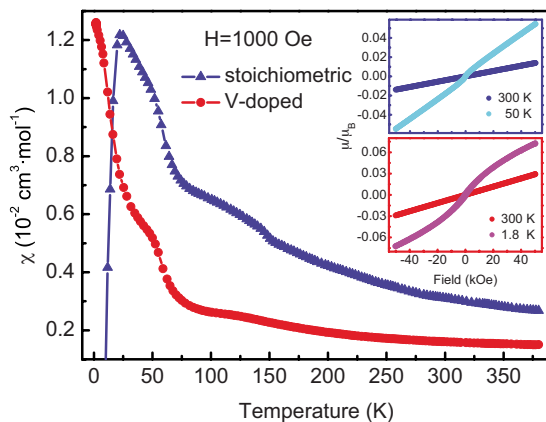

FIG. 2. (Color online) Molar susceptibility of Sr_2VO_3FeAs (blue triangles) and $Sr_2VO_3(Fe_{0.93}V_{0.07})As$ (red circles) at 1 kOe. Insets: hysteresis loops of Sr_2VO_3FeAs (top, blue) and $Sr_2VO_3(Fe_{0.93}V_{0.07})As$ (bottom, red).
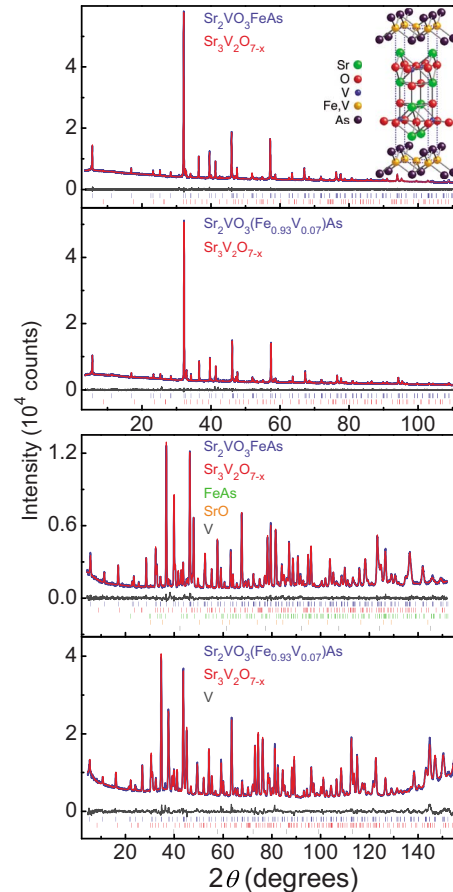
FIG. 3. (Color online) X-ray (top) and neutron (bottom) powder patterns of Sr_2VO_3FeAs and $Sr_2VO_3(Fe_{0.93}V_{0.07})As$ with Rietveld refinements. Inset: crystal structure of Sr_2VO_3FeAs.

powder diffractometer SPODI at FRM II (Garching, Germany) with incident wavelengths of 0.155 nm and 0.146 nm, respectively. Rietveld refinements were performed with the TOPAS package[17] using the fundamental parameter approach as reflection profiles. Vanadium was used as a sample container for the neutron measurements and had to be included in the refinements. In order to describe small peak half width and shape anisotropy effects of the samples, the approach of Le Bail and Jouanneaux[18] was implemented into the TOPAS
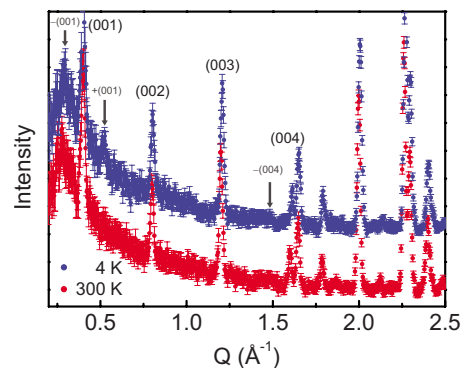

FIG. 4. (Color online) Neutron-powder patterns of Sr_2VO_3FeAs at 4 K (top) and 300 K (bottom). Magnetic reflections are marked arrows.

TABLE I. Crystallographic data of Sr_2VO_3FeAs and $Sr_2VO_3(Fe_{0.93}V_{0.07})As$ at 300 K. $P\frac{4}{n}mm$ (o1).

	Sr_2VO_3FeAs		$Sr_2VO_3(Fe_{0.93}V_{0.07})As$	
Diffractometer	STOE (x-ray)	SPODI (neutron)	STOE (x-ray)	SPODI (neutron)
Wavelength (nm)	0.154	0.155	0.154	0.146
a (pm)[a]	394.58(1)	393.5(1)	393.38(1)	393.1(1)
c (pm)[a]	1573.1(1)	1570(1)	1573.1(1)	1573(1)
V (nm^3)[a]	0.2449(1)	0.243(1)	0.2434(1)	0.243(1)
Z	2	2	2	2
Data points	10650	2955	10650	3029
Reflections[b]	130	196	130	238
Total variables	101	95	94	113
d range	0.941–15.735	0.797–15.700	0.939–15.717	0.749–15.719
R_P, wR_P	0.0147, 0.0196	0.0317, 0.0412	0.0187, 0.0264	0.0321, 0.0405
R_{Bragg}	0.0050	0.0101	0.0044	0.0231
Atomic parameters				
Sr1 $[2c(0,\frac{1}{2},z)]$	$z=0.8100(1)$	$z=0.8096(1)$	$z=0.8096(2)$	$z=0.8092(2)$
	$U_{iso}=131(5)$	$U_{iso}=39(5)$	$U_{iso}=171(6)$	$U_{iso}=49(7)$
Sr2 $[2c(0,\frac{1}{2},z)]$	$z=0.5859(1)$	$z=0.5858(2)$	$z=0.5862(2)$	$z=0.5852(2)$
	$U_{iso}=220(7)$	$U_{iso}=96(6)$	$U_{iso}=239(9)$	$U_{iso}=82(7)$
V/Fe $[2c(0,\frac{1}{2},z)]$	$z=0.3080(3)$	$z=0.306(2)$	$z=0.3086(3)$	$z=0.309(3)$
	$U_{iso}=167(9)$	$U_{iso}=38$[c]	$U_{iso}=179(11)$	$U_{iso}=25$[c]
		Occ. 1.00(1):0.00(1)[d]		Occ. 1.00(1):0.00(1)[d]
Fe/V $[2a(0,0,0)]$	$U_{iso}=134(10)$	$U_{iso}=43(5)$	$U_{iso}=131(13)$	$U_{iso}=40(6)$
	Occ. 0.99(1)[e]	Occ. 0.99(1):0.01(1)[d]	Occ. 1.00(1)[e]	Occ. 0.93(1):0.07(1)[d]
As $[2c(0,\frac{1}{2},z)]$	$z=0.0891(2)$	$z=0.0896(2)$	$z=0.0900(2)$	$z=0.0901(2)$
	$U_{iso}=113(7)$	$U_{iso}=34(6)$	$U_{iso}=178(10)$	$U_{iso}=52(7)$
O1 $[4f(0,0,z)]$	$z=0.2921(4)$	$z=0.2933(1)$	$z=0.2958(5)$	$z=0.2951(1)$
	$U_{iso}=93(19)$[f]	$U_{iso}=56(5)$	$U_{iso}=305(31)$	$U_{iso}=65(7)$
	Occ. 1.00(1)[e]	Occ. 1.00(1)[e]		Occ. 1.00(1)[e]
O2 $[2c(0,\frac{1}{2},z)]$	$z=0.4310(4)$	$z=0.4297(1)$	$z=0.4313(7)$	$z=0.4308(2)$
	$U_{iso}=93(19)$[f]	$U_{iso}=94(8)$	$U_{iso}=419(54)$	$U_{iso}=131(10)$
	Occ. 1.00(1)[e]	Occ. 1.00(1)[e]		Occ. 1.00(1)[e]

[a]Separate refinements without anisotropy parameters.
[b]Main phase.
[c]Restrained as minimum value.
[d]Constrained to a total occupancy of 1.
[e]Restrained to a total occupancy ≤ 1.
[f]U_{iso} of O1 and O2 were refined together.

program and the according parameters were allowed to refine freely. Preferred orientations of the crystallites were described using March Dollase or spherical harmonics functions. The Fe:V ratio at both the iron and the vanadium site was determined by refining the occupancy of the neutron and/or x-ray powder data, oxygen deficiency was ruled out by refining the occupancy of all oxygen sites.

The crystallographic data of Sr_2VO_3FeAs and $Sr_2VO_3(Fe_{0.93}V_{0.07})As$ are compiled in Table I, the powder patterns and Rietveld fits are depicted in Fig. 3. The amounts of impurity phases were determined by quantitative Rietveld analysis. The undoped sample consists of Sr_2VO_3FeAs (89.0 wt %), $Sr_3V_2O_{7-x}$ (7.8 wt %), FeAs (2.9 wt %), and traces of SrO (0.3 wt %), the doped sample consists of $Sr_2VO_3(Fe_{0.93}V_{0.07})As$ (87.3 wt %) and $Sr_3V_2O_{7-x}$ (12.7 wt %) as determined by neutron diffraction. However, the doped sample also shows small amounts of a further, unidentified impurity phase, which could not be included in the refinement. The lattice parameters change only slightly on V doping (a is shortened by 1.2 pm, c is unchanged) but the refinement of the Fe site (neutron data) displays a mixed occupancy of Fe and V in a ratio of 93 ± 1% Fe: 7 ± 1% V in the doped sample. Since the x-ray data give full occupancy of the 2a site (see Table I), we can rule out vacancies at the Fe site and the Fe/V mixing is unambiguous. In contrast to this, the superconducting undoped sample is almost exactly stoichiometric regarding the V, Fe, and O occupancies.

The neutron-powder pattern of undoped, superconducting

Sr_2VO_3FeAs at 4 K shows weak additional peaks at the Q values 0.525, 1.49, and possibly 0.28 Å^{-1}, marked by arrows in Fig. 4. These can be indexed as satellites of the (00ℓ) reflections according to $Q_{(001)}+\Delta Q$, $Q_{(004)}-\Delta Q$, and $Q_{(001)}-\Delta Q$ with $\Delta Q \approx 0.123$ Å^{-1}, respectively. This suggests incommensurate, possibly helical magnetic ordering along the c axis with a propagation vector $\mathbf{q} \approx (0,0,0.306)$ in reciprocal lattice units. Since low-temperature ^{57}Fe-Mössbauer data show no signal splitting,[14] we expect ordering of the V sublattice. This supports the idea of highly correlated vanadium in Sr_2VO_3FeAs, where vanadium d states are removed from the Fermi level by the magnetic exchange splitting. Recent angle-resolved photoemission experiments[19] are in agreement with this model likewise. Even though our data strongly suggest the existence magnetic ordering, we consider them as preliminary. Further experiments in the low-Q region by polarization analysis are required for a precise determination of the magnetic structure and of the temperature dependence of the magnetic order parameter.

In summary, we have shown that Sr_2VO_3FeAs is sensitive to Fe/V mixing in the FeAs layer, which is detrimental to superconductivity. Small V doping of 7%, unambiguously detected by neutron diffraction, suppresses superconductivity completely while the superconducting phase is nearly stoichiometric. We suggest that even smaller Fe/V inhomogeneities are intrinsic in this material and may be responsible for the scattered critical temperatures and superconducting phase fractions reported in the literature. Small but significant additional reflections emerge in the neutron-powder pattern of superconducting Sr_2VO_3FeAs at 4 K. A preliminary analysis indicates incommensurable, possibly helical magnetic ordering of the V moments with a propagation vector $\mathbf{q} \approx (0,0,0.306)$. This is in agreement with strongly correlated vanadium, which does not significantly contribute to the Fermi surface. Thus, Sr_2VO_3FeAs fits to the other iron pnictide superconductors and represents no new paradigm, although the absence of iron magnetism and possible self-doping effects remain open questions.

---

*johrendt@lmu.de

[1] Y. Kamihara, T. Watanabe, M. Hirano, and H. Hosono, J. Am. Chem. Soc. **130**, 3296 (2008).

[2] M. Rotter, M. Tegel, and D. Johrendt, Phys. Rev. Lett. **101**, 107006 (2008).

[3] X. C. Wang, Q. Q. Liu, Y. X. Lv, W. B. Gao, L. X. Yang, R. C. Yu, F. Y. Li, and C. Q. Jin, Solid State Commun. **148**, 538 (2008).

[4] I. Mazin and M. D. Johannes, Nat. Phys. **5**, 141 (2009).

[5] C. de la Cruz, Q. Huang, and J. W. Lynn, Nature (London) **453**, 899 (2008).

[6] D. R. Parker, M. J. Pitcher, P. J. Baker, I. Franke, T. Lancaster, S. J. Blundell, and S. J. Clarke, Chem. Commun. (Cambridge) 2009, 2189.

[7] M. Rotter, M. Tegel, D. Johrendt, I. Schellenberg, W. Hermes, and R. Pöttgen, Phys. Rev. B **78**, 020503(R) (2008).

[8] I. I. Mazin, D. J. Singh, M. D. Johannes, and M. H. Du, Phys. Rev. Lett. **101**, 057003 (2008).

[9] H. Ogino, Y. Katsura, S. Horii, K. Kishio, and J. Shimoyama, Supercond. Sci. Technol. **22**, 085001 (2009).

[10] M. Tegel, F. Hummel, S. Lackner, I. Schellenberg, R. Pöttgen, and D. Johrendt, Z. Anorg. Allg. Chem. **635**, 2242 (2009).

[11] X. Y. Zhu, F. Han, G. Mu, P. Cheng, B. Shen, B. Zeng, and H. H. Wen, Phys. Rev. B **79**, 220512 (2009).

[12] K. W. Lee and W. E. Pickett, EPL **89**, 57008 (2010).

[13] I. I. Mazin, Phys. Rev. B **81**, 020507 (2010).

[14] G. Cao, Z. Ma, C. Wang, Y. Sun, J. Bao, S. Jiang, Y. Luo, C. Feng, Y. Zhou, Z. Xie, F. Hu, S. Wei, I. Nowik, I. Felner, L. Zhang, Z. Xu, and F. Zhang, Phys. Rev. B **82**, 104518 (2010).

[15] A. Pal, A. Vajpayee, R. S. Meena, H. Kishan, and V. P. S. Awana, J. Supercond. Novel Magn. **22**, 619 (2009).

[16] M. Tegel, F. Hummel, Y. Su, T. Chatterji, M. Brunelli, and D. Johrendt, EPL **89**, 37006 (2010).

[17] A. Coelho, TOPAS-ACADEMIC, version 4.1, Coelho Software, Brisbane, 2007.

[18] A. Le Bail and A. Jouanneaux, J. Appl. Crystallogr. **30**, 265 (1997).

[19] T. Qian, N. Xu, Y. Shi, K. Nakayama, P. Richard, T. Kawahara, T. Sato, T. Takahashi, M. Neupane, Y. Xu, X. Wang, G. Xu, X. Dai, Z. Fang, P. Cheng, H. Wen, and H. Ding, arXiv:1008.4905 (unpublished).